Liquid Crystals
Publication details, including instructions for authors and subscription information:
http://www.informaworld.com/smpp/title~content=t713926090

Liquid crystalline behaviour of benzoic acid derivatives containing alkoxyazobenzene

Binglian Bai[a]; Haitao Wang[a]; Hong Xin[a]; Beihong Long[a]; Min Li[a]
[a] Key Laboratory for Automobile Materials (JLU), Ministry of Education, Institute of Materials Science and Engineering, Jilin University, Changchun 130012, P. R. China

To cite this Article Bai, Binglian , Wang, Haitao , Xin, Hong , Long, Beihong and Li, Min(2007) 'Liquid crystalline behaviour of benzoic acid derivatives containing alkoxyazobenzene', Liquid Crystals, 34: 6, 659 — 665
To link to this Article: DOI: 10.1080/02678290701328118
URL: http://dx.doi.org/10.1080/02678290701328118

Liquid Crystals, Vol. 34, No. 6, June 2007, 659–665

Liquid crystalline behaviour of benzoic acid derivatives containing alkoxyazobenzene

BINGLIAN BAI, HAITAO WANG, HONG XIN, BEIHONG LONG and MIN LI*

Key Laboratory for Automobile Materials (JLU), Ministry of Education, Institute of Materials Science and Engineering, Jilin University, Changchun 130012, P. R. China

(*Received 4 December 2006; accepted 14 February 2007*)

Liquid crystal trimers based on the hydrogen bonding dimerization of 4-{n-[4-(4-m-alkoxyphenylazo)phenoxy]alkoxy}benzoic acid (**BAm-n**) have been synthesized and characterized. Temperature-dependent FTIR spectroscopic studies showed that the carboxylic acid groups in **BAm-n** are associated to form H-bonded cyclic dimers both in their crystalline and liquid crystalline phases. The trimers exhibited enantiotropic liquid crystalline behaviour except for **BA1-3** which showed monotropic behaviour, and the mesophases changed from nematic to smectic phase, with the increase of length of the spacer and the terminal substituents. Pronounced odd–even effects in the melting temperatures, clearing temperatures and nematic–isotropic enthalpy changes were observed.

1. Introduction

Liquid crystal dimers [1, 2] consisting of two identical (symmetric) or non-identical (non-symmetric) mesogenic units have attracted much attention as they have been recognized as model compounds for main-chain [3] and side-chain liquid crystalline polymers [4]. More recently, in order to investigate how the liquid crystals properties evolve from dimers to polymers, a range of higher oligomers have been prepared and characterized. Imrie and Luckhurst [5] extensively investigated the liquid crystal trimers, namely, the 4,4′-bis[ω-(4-cyanobiphenyl-4′-yloxy)alkoxy]biphenyls. They confirmed that the nematic–isotropic transition temperatures and the associated entropy changes exhibited a dramatic odd–even effect as the length and parity of the spacers was varied, in which the even members exhibited higher values. Recently, they found for the first time that non-symmetric liquid crystal trimers exhibited a new smectic modification, the triply-intercalated alternating smectic C phase [6]. Different types of liquid crystal trimers have been reported, such as symmetrical [7] or unsymmetrical trimers [8–12] in which the mesogenic units are linked by spacers of equal or different lengths. To date, however, among the reported liquid crystalline trimers, the mesogenic groups are generally covalently linked by two flexible spacers.

It is well known that hydrogen bonding is one of the key interactions for chemical and biological processes in nature due to its stability, directionality and dynamics, and it plays an important role in inducing or stabilizing liquid crystallinity. Over the last two decades, a number of supramolecular mesogenic materials have been obtained through intermolecular hydrogen bonding. A typical example are the 4-alkoxybenzoic acids, which show liquid crystalline behaviour due to dimerization of the acids through hydrogen bonding between -C=O and -OH [13]. Kato and Fréchet [14] expanded this identical component concept to include mixtures of differing components and obtained liquid crystals from binary mixtures of 4-alkoxybenzoic acids and pyridine-based derivatives. Such a study provides excellent examples of specific molecular recognition. After that, Kato *et al.* [15–18] and Brienne *et al.* [19] reported a series of thermotropic supramolecular liquid crystals obtained by molecular recognition processes through intermolecular hydrogen bonds. Although much attention has been paid to hydrogen bonded supramolecular liquid crystals in recent years, and even many liquid crystal dimers based on the hydrogen bonding interactions have been studied [20–22], little attention has been paid to the supramolecular liquid crystal trimers based on hydrogen bonding interactions [23, 24].

Our present work reports the design and synthesis of a series of supramolecular liquid crystal trimers containing 4-alkoxyazobenzene groups and H-bonded benzoic acid as mesogenic units (see scheme 1), and investigation of the influence of length of both spacers and terminal chains on the mesophase behaviour to understand structure–property relationships.

*Corresponding author. Email: minli@jlu.edu.cn

Liquid Crystals
ISSN 0267-8292 print/ISSN 1366-5855 online © 2007 Taylor & Francis
http://www.tandf.co.uk/journals
DOI: 10.1080/02678290701328118

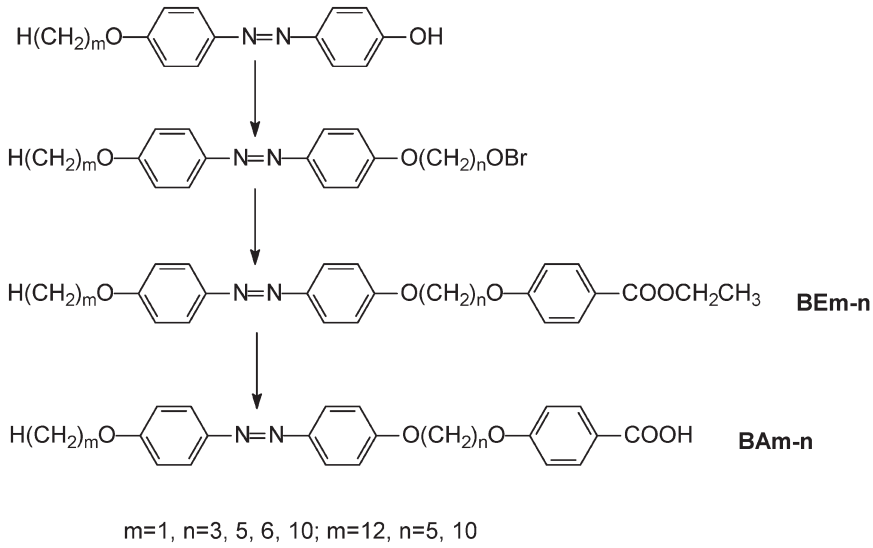

Scheme 1. The synthesis of **BAm-n**.

2. Experimental

2.1. *Synthesis*

The compounds, 4-{n-[4-(4-m-alkoxyphenylazo)phenoxy]alkoxy}benzoic acid (**BAm-n**), were synthesized by the route shown in scheme 1. The syntheses of **BE1-3**, **BE1-5**, **BE1-6** and **BE1-10** are reported elsewhere [25]; similarly, **BE12-5** and **BE12-10** were synthesized and characterized. The target products (**BAm-n**) were obtained through hydrolysis of **BEm-n** and were purified through recrystallization from DMF for further ^{1}H NMR measurements, FTIR and elemental analysis. (Because of its poor solubility, the ^{1}H NMR measurement of **BA12-10** was not performed).

2.1.1. 4-{5-[4-(4-dodecyloxyphenylazo)phenoxy]pentyloxy}benzoic acid ethyl ester (BE12-5). Yield, 77.68%. ^{1}H NMR (300 MHz, $CDCl_3$), (ppm, from TMS): 0.87–0.90 (t, 3H, -O-$(CH_2)_{11}$-$\underline{CH_3}$), 1.27–1.39 (m, 19H, -O-C-C-C-$\underline{(CH_2)_8}$-CH_3 and -$\underline{COO}$-CH_2-$\underline{CH_3}$), 1.46–1.49 (m, 2H, -O-C-C-$\underline{CH_2}$-$(CH_2)_8$-CH_3), 1.68–1.71 (m, 2H, -O-C-C-CH_2-C-C-O), 1.79–1.83 (m, 2H, -O-C-$\underline{CH_2}$-$(CH_2)_9$-CH_3), 1.89–1.92 (m, 4H, -O-C-CH_2-C-CH_2-C-O), 4.02–4.09 (m, 6H, -O-CH_2-C-), 4.32–4.37 (m, 2H, -COO-$\underline{CH_2}$-CH_3), 6.90–6.92 (d, 2H, Ar-H, m-to, -COO-), 6.98–7.00 (d, 4H, Ar-H, m-to, -N=N-), 7.89–7.90 (d, 4H, Ar-H, o-to, -N=N-), 7.98–8.00 (d, 2H, Ar-H, o-to, -COO-). FTIR (KBr, pellet, cm^{-1}): 2924, 2854, 1709, 1602, 1580, 1495, 1474, 1317, 1289, 1246, 1174, 1147, 1108, 1020, 849, 768, 720. Elemental analysis: found C 74.24, N 4.54, H 8.76%; calcd. for $C_{38}H_{52}N_2O_5$ C 73.99, N 4.54, H 8.50%. For compound **BE12-10**, elemental analysis: found C 75.44, N 4.00, H 9.43%; calcd. for $C_{43}H_{62}N_2O_5$ C 75.18, N 4.08, H 9.10%.

2.1.2. 4-{5-[4-(4-dodecyloxyphenylazo)phenoxy]pentyloxy}benzoic acid (BA12-5). 2.97 g (0.0048 mol) of BE12-5 was dissolved in the mixture of tetrahydrofuran and anhydrous alcohol (400 ml), an excess amount of potassium hydroxide was added (8 g), and then the resulting mixture was stirred under reflux for 20 h. The reaction mixture was poured into an excess of ice water and maintained the pH<7 by adding hydrochloric acid, and the precipitate was recrystallized from DMF; yield, 80.76%. ^{1}H NMR (300 MHz, DMSO), (ppm, from TMS): 0.83–0.87 (t, 3H, -O-$(CH_2)_{11}$-$\underline{CH_3}$), 1.24–1.43 (m, 18H, -O-C-C-$\underline{(CH_2)_9}$-CH_3), 1.60–1.62 (m, 2H, -O-C-C-CH_2-C-C-O), 1.71–1.76 (m, 2H, -O-C-$\underline{CH_2}$-$(CH_2)_9$-CH_3), 1.80–1.86 (m, 4H, -O-C-CH_2-C-CH_2-C-O), 4.04–4.12 (m, 6H, -O-CH_2-C-), 7.00–7.03 (d, 2H, Ar-H, m-to, -COOH), 7.07–7.11 (d, 4H, Ar-H, m-to, -N=N-), 7.80–7.85 (d, 4H, Ar-H, o-to, -N=N-), 7.86–7.89 (d, 2H, Ar-H, o-to, -COOH), 12.63 (s, 1H, -COOH). FTIR (KBr, pellet, cm^{-1}): 3069, 2919, 2850, 2680, 2558, 1703, 1684, 1603, 1581, 1497, 1435, 1395, 1320, 1298, 1249, 1176, 1152, 1109, 1065, 947, 852, 840, 771, 720. Elemental analysis: found C 73.82, N 4.76, H 8.42%; calcd. for $C_{36}H_{48}N_2O_5$ C 73.44, N 4.76, H 8.22%.

Using the same method, compounds **BA12-10**, **BA1-3**, **BA1-5** and **BA1-10** were successfully synthesized and their structures were confirmed by IR and ^{1}H NMR spectroscopy. **BA12-10** elemental analysis: found C 74.79, N 4.20, H 8.98%; calcd. for $C_{41}H_{58}N_2O_5$ C 74.74, N 4.25, H 8.87%. **BA1-3** elemental analysis: found C 67.62, N 6.56, H 5.24%; calcd. for $C_{23}H_{22}N_2O_5$

C 67.97, N 6.89, H 5.46%. **BA1-5** elemental analysis: found C 69.35, N 6.39, H 6.03%; calcd. for $C_{25}H_{26}N_2O_5$ C, 69.11; N, 6.45; H, 6.03%. **BA1-6** elemental analysis: found C 69.50, N 5.95, H 6.28%; calcd. for $C_{26}H_{28}N_2O_5$ C 69.63, N 6.25, H 6.29%. **BA1-10** elemental analysis: found C 71.33, N 5.24, H 7.13%; calcd. for $C_{30}H_{36}N_2O_5$ C 71.40, N 5.55, H 7.19%.

2.2. *Characterization*

^{1}H NMR spectra were recorded with a Mercury-300BB 300 MHz spectrometer, using DMSO-*d*6 as solvent and tetramethylsilane (TMS) as an internal standard. FTIR spectra were recorded with a Perkin–Elmer spectrometer (Spectrum One B). The sample was pressed tablet with KBr. The thermal properties of the compounds were investigated with a Mettler-Toledo DSC821^e instrument. The rate of heating and cooling was 10°C min^{-1}; the weight of the sample was about 2 mg, and indium and zinc were used for calibration. The peak maximum was taken as the phase transition temperature. Optical textures were observed under a Leica DMLP microscope equipped with a Leitz 350 heating stage. X-ray diffraction (XRD) was measured with a Bruker Avance D8 X-ray diffractometer.

3. Results and discussion

3.1. *Hydrogen bonding associations in the phases*

To investigate the intermolecular hydrogen bonding between -COOH groups in **BAm-n**, FTIR spectra were measured at various temperatures. Figure 1 shows the FTIR spectra of compound **BA12-10** in the range from 1780 cm^{-1} to 1650 cm^{-1} at different temperatures. Generally, the stretching vibration of free C=O in carboxylic acids appears at 1737 cm^{-1} [26–32], whereas that of the H-bonded C=O from the H-bonded cyclic dimers is at 1683 and 1677 cm^{-1} [28–30]. It can be seen that both free (1732 cm^{-1}) and H-bonded C=O (1692 cm^{-1}) are observed in the isotropic phase of **BA12-10**, although both the relative intensity and its wavenumber of H-bonded C=O groups decrease with a decrease of temperature. In contrast, all the C=O groups are H-bonded within the SmC and SmF phases, with their appearance at 1686 cm^{-1} slowly shifting to 1679 cm^{-1} upon decreasing temperature. Two H-bonded C=O groups centred at 1703 and 1679 cm^{-1} are detected in the crystalline phase of **BA12-10**; usually the existence of two different frequencies indicate the strengths of the H-bonds holding the two acid molecules together are different, as observed in the present case.

The percentage of H-bonded -COOH groups versus temperature is plotted in figure 2. The percentage of H-bonded -COOH groups was determined by the equation of [(area of H-bonded $\nu_{C=O}$)/(total Area of $\nu_{C=O}$)] × 100% [29]. It is clear from the above FTIR analysis, that all the carboxylic acid groups in **BA12-10** are associated to form H-bonded cyclic dimers either in its crystalline or in its smectic phases (scheme 2). Temperatur- dependent IR spectroscopic investigation of **BA12-5** and **BA1-10** gave similar results to that for **BA12-10**.

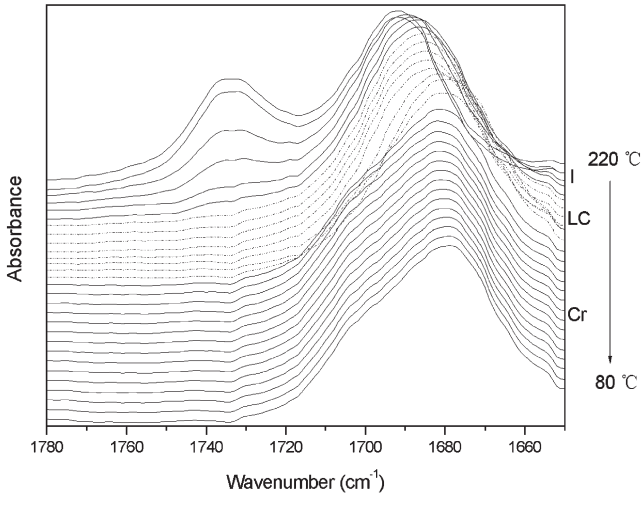

Figure 1. FTIR spectra of **BA12-10** in the range 1780–1650 cm^{-1} at intervals of 5°C on cooling from 220 to 80°C.

3.2. *Phase behaviour of BEm-n and BAm-n*

3.2.1. The BEm-n series. The transitional temperatures and associated enthalpies for the **BEm-n** series are summarized in table 1. Apart from **BE1-3** and **BE1-5**,

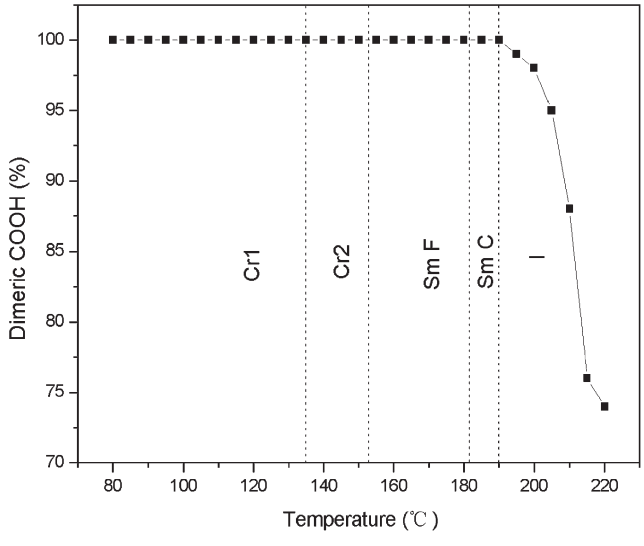

Figure 2. Molar percentage of H-bonded -COOH of **BA12-10** versus temperature on cooling.

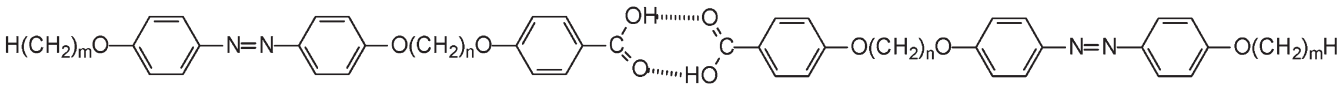

Scheme 2. Liquid crystal trimers based on H-bonded cyclic dimers.

which are non-mesomorphic, all the members of **BEm-n** exhibit monotropic liquid crystalline behaviour. Schlieren texture was observed for **BE1-6** and **BE1-10** indicating a nematic phase. Both **BE12-5** and **BE12-10**, which have long alkyl terminal chains, exhibit a smectic A phase, which showed typical fan-like texture (figure 3 a) and a tilted mesophase (SmC phase) on cooling. The SmA–SmC transition was evidenced by the fact that the focal conic fan-like texture became broken and coarse and gave a Schlieren texture on shearing (figure 3 b).

The XRD pattern of **BE12-5** in the SmA phase consists of a broad diffuse peak in the wide-angle region and two orders of reflections in the low-angle region, corresponding to a layer spacing of d=41.96 Å at 100°C (SmA phase), which shrank to d=41.56 Å measured at 78°C in the SmC phase. We notice that the change in layer spacing upon going from SmA to SmC is only 0.4 Å, which is small and lies in the range of the experimental error and hence, it is not possible to confirm the transition of SmA to SmC based on these XRD data. However, the SmA–SmC transition was confirmed by the textural change observed via polarizing optical microscope. As we have already noted, the focal conic fan-like texture in the smectic A phase of **BA12-5** became pseudo-isotropic region on shearing, which turned to a Schlieren texture within the smectic C phase. The apparently lack of decrease in the layer spacing arises probably because at the transition from SmA to SmC only the tilt angle direction distribution function changes, and this will not affect the layer spacing [33]. A similar phase sequence was observed for **BE12-10** (the region of SmC phase is too narrow to be detected by XRD). The layer spacing values are collected in table 2. The XRD pattern of **BE12-5** at 69°C exhibited four sharp peaks at 2θ=2.20° (the first-order diffraction), 4.35° (the second-order diffraction), 6.58° (the third-order diffraction) and 8.76° (the fourth-order diffraction) in the low-angle region and a new peak at 2θ=24.34° (d=3.65 Å) and a weak diffuse peak centred at a spacing of 4.4 Å in the wide-angle region, which indicates that **BE12-5** exhibits a high-ordered layered structure (SmX).

3.2.2. BAm-n series. Almost all **BAm-n** compounds exhibit enantiotropic liquid crystalline behaviour, except for **BA1-3** which is monotropic. The transitional temperatures and the associated enthalpies for the **BAm-n** series are presented in table 1. Compounds **BA1-3**, **BA1-5** and **BA1-6** exhibit characteristic nematic Schlieren texture (figure 3 c).

The XRD pattern of **BA12-10** at 185°C (figure 4 a) consists of a sharp peak (d=71.19 Å), which is shorter than the calculated length (l=94.20 Å) of hydrogen bonding dimer, suggesting its SmC characteristic. The XRD patterns for **BA12-10** between 153°C and 181°C showed three orders of reflection in the low-angle region, implying the formation of well-defined smectic layer structures, and a weak sharp peak in the wide-angle region with a spacing of 4.50 Å (2θ=19.70°).

Table 1. Transition temperatures (°C) and enthalpies (kJ mol^{-1}, in parentheses) of **BEm-n** and **BAm-n**.

Compound	First cooling	Second heating
BA12-10	I 188 (26.3) SmC 181 (6.6) SmF 153 (16.0) Cr2 135 (21.4) Cr1	Cr1 150 (21.5) Cr2 158 (16.9) SmF 183 (6.1) SmC 191 (24.0) I
BA12-5	I 194 (16.0) SmC 168 (13.4) Cr 161 (14.1) Cr	Cr 170 (28.5) SmC 196 (15.5) I
BA1-10	I 206 (22.0) SmC 163 (30.5) Cr 153 (17.9) Cr	Cr 176 (6.2) Cr 184 (50) SmC 210 (19.3) I
BA1-6	I 239 (18.8) N 186 (40.5) Cr 157 (2.2) Cr	Cr 174 (4.3) Cr 212 (41.9) N 242 (19.3) I
BA1-5	I 213 (5.4) N 158 (37.4) Cr	Cr 190 (41.9) N 214 (5.7) I
BA1-3	I 203 (3.9) N 180 (43.8) Cr	Cr 225 (1.9) Cr 229 (48.5) I
BE12-10	I 115 (15.9) SmA 103 (4.1) SmC 100 (37.1) Cr	Cr 119 (81.9) I
BE12-5	I 106 (8.4) SmA 85[b] SmC 72 (12.7)SmX 64 (6.6) Cr	Cr 71 (8.3)[a] Cr 108 (53.3) I
BE1-3	I 92 (39.9) Cr	Cr 131 (42.1) I
BE1-5	I 98 (42.2) Cr	Cr 129 (47.8) I
BE1-6	I 132 (3.2) N 115 (52.6) Cr	Cr 131 (64.3) I
BE1-10	I 109 (0.1) N 108 (82.0) Cr	Cr 127 (90.9) I

Cr, SmA, SmC, SmF, SmX and I indicate crystalline state, smectic A phase, smectic C phase, smectic F phase, smectic X phase and isotropic liquid, respectively. [a]Exothermic peak; [b]not detected by DSC.

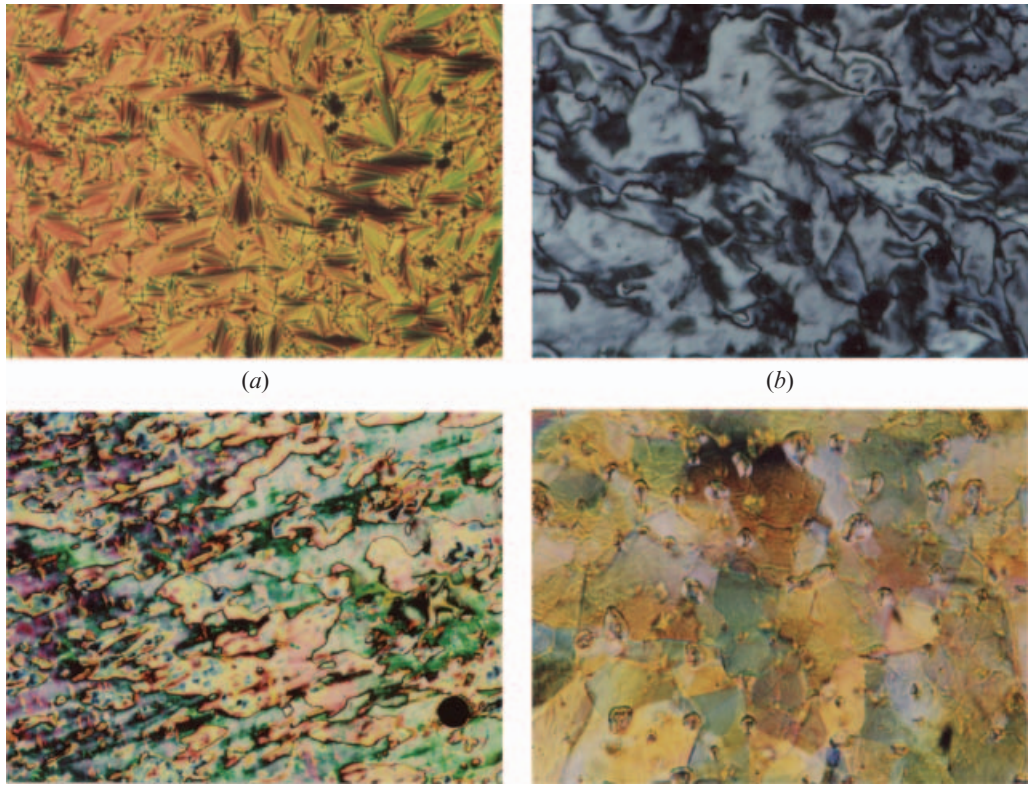

Figure 3. Polarizing optical photomicrograph of (a) **BE12-5** at 94.7°C (×200); (b) **BE12-5** at 78°C (×200); (c) **BA1-5** at 182°C (×200); (d) **BA12-10** at 175°C (×400).

Thus the phase is assigned to smectic F, which is consistent with the Schlieren-mosaic texture (figure 3 d) [34]. As can be seen from figures 4 c and 4 d, it is apparent that the crystal structure changes during the transition from Cr_1 to Cr_2 for **BA12-10**. Both **BA12-5** and **BA1-10** exhibit monolayer SmC behaviour. Appropriate values of *d*, *l* and *d*/*l* ratios are collected in table 2.

Both the length and parity of the flexible spacers in these hydrogen bonded supramolecular liquid crystal trimers play an important role, as observed in liquid crystalline trimers based on covalent bonds [5, 6]. The melting and clearing points as well as the nematic–isotropic enthalpy changes of **BA1-5** are much lower than those of **BA1-6**, showing an obvious odd–even effect. Compared to that of **BA1-6**, the melting point and clearing points of **BA1-10** decrease, and the liquid crystalline phase changes from nematic to smectic phase, with the increase of length of the spacer. It can readily be seen from table 1 that the length of terminal substituents plays an important role in the formation and stabilization of the smectic phase. For example,

Table 2. Summary of X-ray diffraction results for **BEm-n** and **BAm-n** in the mesophase.

Compound	Molecular length[a] *l*/Å	*T*/°C (cooling)	Layer spacing *d*/Å	*d*/*l*
BE12-5	44.17	100 (SmA)	41.96	0.95
		78 (SmC)	41.56	0.94
		69 (SmX)	40.12	0.91
BE12-10	51.03	112 (SmA)	48.52	0.95
BA12-5	81.40	185 (SmC)	60.48	0.74
BA12-10	94.20	185 (SmC)	71.19	0.76
		175 (SmF)	76.75	0.81
BA1-10	69.06	180 (SmC)	60.86	0.88

[a]Molecular length was calculated by MM1 and the calculated length of **BAm-n** is the length of hydrogen bonding dimers.

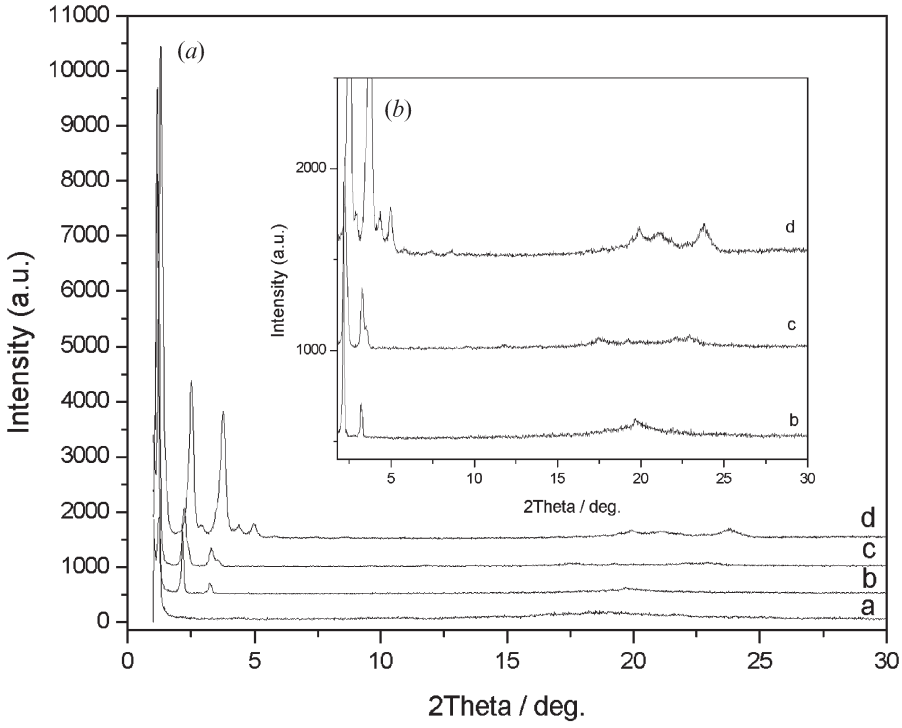

Figure 4. (A) X-ray diffraction pattern of **BA12-10** at 185°C (a), 175°C (b), 145°C (c), 55°C (d) on cooling; (B) is the expanded picture of (A).

compared with that of **BA1-5**, which showed a nematic phase, **BA12-5** exhibited smectic behaviour, indicating that the smectic phase can be stabilized by elongation of the terminal substituents (because of only two types of terminal substituents synthesized, we can not conclude generality). This phenomenon could be understood in terms of the microphase segregation effect being increased due to the increase of the incompatibility between the rigid aromatic rings and flexible alkoxy chains with the increase of length of the terminal alkyl chains. The microsegregation effect was considered to be the driving force for the formation of smectic phase. Additionally, the melting point, clearing point, as well as the enthalpy changes of LC trimers (**BAm-n**) are much higher, and mesophase ranges are broader than that of the corresponding **BEm-n**, suggesting that the molecular arrangement of LC trimers is more stable due to the dimerization between -COOH groups.

4. Conclusion

In summary, novel liquid crystal trimers based on the hydrogen bonding dimerization containing 4-alkoxyazobenzene group have been synthesized and characterized. All the carboxylic acid groups in **BAm-n** are associated to form the H-bonded cyclic dimers either in crystalline and liquid crystalline phase, and due to the formation of H-bonded cyclic dimers, the liquid crystalline phase of LC trimers (**BAm-n**) is more stable than that of the corresponding **BEm-n**. The lengths and parity of the flexible spacers as well as the terminal alkyl chains play key roles in stabilization and formation of liquid crystalline phases in H-bonded liquid crystal trimers.

Acknowledgements

The authors are grateful to the National Science Foundation Committee of China (project No. 50373016), Program for New Century Excellent Talents in Universities of China Ministry of Education, Special Foundation for PhD Program in Universities of China Ministry of Education (Project No. 20050183057) and Project 985-Automotive Engineering of Jilin University for their financial support of this work.

References

[1] C.T. Imrie, G.R. Luckhurst. *Handbook of Liquid Crystals*, Vol. 2B, D. Demus, J.W. Goodby, G.W. Gray, H.W. Spiess, V. Vill (Eds), p. 801, Wiley-VCH, Weinheim (1998).

[2] C.T. Imrie, P.A. Henderson. *Curr. Opin. Colloid. Inter. Sci.*, **7**, 298 (2002).

[3] (a) A.C. Griffin, T.R. Britt. *J. Am. chem. Soc.*, **103**, 4957 (1981); (b) J.C.W. Chien, R. Zhou, C.P. Lillya. *Macromolecules*, **20**, 2340 (1987).
[4] (a) C.T. Imrie, F.E. Karasz, G.S. Attard. *Macromolecules*, **26**, 545 (1993); (b) C.T. Imrie, F.E. Karasz, G.S. Attard. *Macromolecules*, **26**, 3803 (1993).
[5] C.T. Imrie, G.R. Luckhurst. *J. Mater. Chem.*, **8**, 1339 (1998).
[6] (a) C.T. Imrie, P.A. Henderson, J.M. Seddon. *J. Mater. Chem.*, **14**, 2486 (2004); (b) P.A. Henderson, C.T. Imrie. *Liq. Cryst.*, **32**, 673 (2005).
[7] A.T.M. Marcelis, A. Koudijs, E.J.R. Sudholter. *Mol. Cryst. liq. Cryst.*, **330**, 1289 (1999).
[8] (a) C.V. Yelamaggad, U.S. Hiremath, D.S. Shankar Rao, S. Krishna Prasad. *Chem. Commun.* 57 (2000); (b) C.V. Yelamaggad, S. Anitha nagamani, U.S. Hiremath, D.S. Shankar Rao, S. Krishna Prasad. *Liq. Cryst.*, **28**, 1581 (2001).
[9] (a) D. Hölter, H. Frey, R. Mülhaupt, J.E. Klee. *Adv. Mater.*, **10**, 864 (1998); (b) A.C. Sentman, D.L. Gin. *Adv. Mater.*, **13**, 1398 (2001).
[10] I. Nishiyama, J. Yamamoto, J.W. Goodby, H. Yokoyama. *J. Mater. Chem.*, **13**, 2429 (2003).
[11] S. Kumar, M. Manickam. *Liq. Cryst.*, **26**, 939 (1999).
[12] S. Mahlstedt, D. Janietz. *Liq. Cryst.*, **26**, 1359 (1999).
[13] G.W. Gray, B. Jone. *J. chem. Soc.*, 1467 (1954).
[14] T. Kato, J.M.J. Fréchet. *J. Am. chem. Soc.*, **111**, 8533 (1989).
[15] T. Kato, A. Fujishima, J.M.J. Fréchet. *Chem. Lett.*, 919 (1990).
[16] T. Kato, T. Uryu, F. Kaneuchi, C. Jin, J.M.J. Fréchet. *Liq. Cryst.*, **14**, 1311 (1993).
[17] T. Kato, J.M.J. Fréchet, P.G. Wilson, T. Saito, T. Uryu, A. Fujishima, C. Jin, F. Kaneuchi. *Chem. Mater.*, **5**, 1094 (1993).
[18] H. Kihara, T. Kato, T. Uryu, J.M.J. Fréchet. *Chem. Mater.*, **8**, 961 (1996).
[19] M.-J. Brienne, J. Gabrad, J.-M. Lehn, I. Stibor. *J. chem. Soc., Chem. Commun.*, 1868 (1989).
[20] M.J. Wallage, C.T. Imrie. *J. Mater. Chem.*, **7**, 1163 (1997).
[21] J.W. Lee, J.I. Jin, M.F. Achard, F. Hardouin. *Liq. Cryst.*, **28**, 663 (2001).
[22] C.M. Paleos, D. Tsiourvas. *Liq. Cryst.*, **28**, 1127 (2001).
[23] A. Takahashi, V.A. Mallia, N. Tamaoki. *J. Mater. Chem.*, **13**, 1582 (2003).
[24] B.L. Bai, D.M. Pang, M. Li. *Chem. J. Chin. Universities*, **26**, 1957 (2005).
[25] B.L. Bai, M. Li, D.M. Pang, Y.Q. Wu, H.H. Zhang. *Liq. Cryst.*, **32**, 755 (2005).
[26] R.-Q. Zheng, E.-Q. Chen, S.Z.D. Cheng, F. Xie, D. Yan, T. He, V. Percec, P. Chu, G. Ungar. *Macromolecules*, **32**, 3574 (1999).
[27] S.G. Stepanian, I.D. Reva, E.D. Radchenko, G.G. Sheina. *Vib. Spectrosc.*, **11**, 123 (1996).
[28] S. Kutsumizu, R. Kato, M. Yamada, S. Yano. *J. phys. Chem. B*, **101**, 10666 (1997).
[29] K.U. Jeong, S. Jin, J.J. Ge, B.S. Knapp, M.J. Graham, J. Ruan, M.M. Guo, H.M. Xiong, F.W. Harris, S.Z.D. Cheng. *Chem. Mater.*, **17**, 2852 (2005).
[30] J. Dong, Y. Ozaki, K. Nakashima. *Macromolecules*, **30**, 1111 (1997).
[31] S.I. Torgova, M.P. Petrov, A. Strigazzi. *Liq. Cryst.*, **28**, 1439 (2001).
[32] S. Kutsumizu, M. Yamada, T. Yamaguchi, K. Tanaka, R. Akiyama. *J. Am. chem. Soc.*, **125**, 2858 (2003).
[33] G.S. Attard, R.W. Date, C.T. Imrie, G.R. Luckhurst, S.J. Roskilly, J.M. Seddon, L. Taylor. *Liq. Cryst.*, **16**, 529 (1994).
[34] G.W. Gray, J.W.G. Goodby. *Smectic Liquid Crystals – Textures and Structures*, p. 94, Leonard Hill, (1984).